New BIOTECHNOLOGY 69 (2022) 36–48

Contents lists available at ScienceDirect

New BIOTECHNOLOGY

journal homepage: www.elsevier.com/locate/nbt

Affinity-based isolation of extracellular vesicles by means of single-domain antibodies bound to macroporous methacrylate-based copolymer

Lidija Filipović [a], Milica Spasojević [a], Radivoje Prodanović [b], Aleksandra Korać [c], Suzana Matijaševic [c], Goran Brajušković [c], Ario de Marco [d], Milica Popović [b,*]

[a] Innovative Centre of the Faculty of Chemistry, Belgrade, Serbia
[b] University of Belgrade-Faculty of Chemistry, Belgrade, Serbia
[c] University of Belgrade-Faculty of Biology, Belgrade, Serbia
[d] Laboratory for Environmental and Life Sciences, University of Nova Gorica, Nova Gorica, Slovenia

ARTICLE INFO

Keywords:
Nanobodies
Extracellular vesicles
Exosomes
Methacrylate-based copolymer
Immunopurification

ABSTRACT

Correct elucidation of physiological and pathological processes mediated by extracellular vesicles (EV) is highly dependent on the reliability of the method used for their purification. Currently available chemical/physical protocols for sample fractionation are time-consuming, often scarcely reproducible and their yields are low. Immuno-capture based approaches could represent an effective purification alternative to obtain homogeneous EV samples. An easy-to-operate chromatography system was set-up for the purification of intact EVs based on a single domain (VHH) antibodies-copolymer matrix suitable for biological samples as different as conditioned cell culture medium and human plasma. Methacrylate-based copolymer is a porous solid support, the chemical versatility of which enables its efficient functionalization with VHHs. The combined analyses of morphological features and biomarker (CD9, CD63 and CD81) presence indicated that the recovered EVs were exosomes. The lipoprotein markers APO-A1 and APO-B were both negative in tested samples. This is the first report demonstrating the successful application of spherical porous methacrylate-based copolymer coupled with VHHs for the exosome isolation from biological fluids. This inexpensive immunoaffinity method has the potential to be applied for the isolation of EVs belonging to different morphological and physiological classes.

Introduction

Extracellular vesicles (EVs) are cell-secreted supramolecular structures. Their classification is typically based on multiple properties, including the process of biogenesis, density, dimension and the expression of specific biomarkers [1]. Based on their mechanism of release and size, EVs are categorized as exosomes (EXO), microvesicles/shedding particles, and apoptotic bodies. Their content differs according to the characteristics of the cells from which they originated. Microvesicles and apoptotic bodies are released directly from the plasma membrane in living or dying cells, whereas EXOs are released after the fusion of late endosomes with the plasma membrane [2]. Apoptotic bodies are the largest of the EVs, followed by microvesicles, while the smallest are EXOs, the diameter of which measures between 150 and 20 nm and which are present in any biological fluid (blood, urine, cerebrospinal fluid, milk, ascites) [2]. Initially, it was believed that EXOs represented an alternative means of eliminating waste products, but later their role in intercellular communication emerged [3]. This awareness promoted the efforts aimed at elucidating their physiological and pathological significance [4] and, in parallel, evaluating their potential as diagnostic [5] and therapeutic agents [6]. Proteomic studies performed on EXOs from different sources such as primary cells, cell cultures, tissue cultures or biological fluids, identified common biomarkers, as well as proteins and modified epitopes specifically related to vesicle cellular origin and physiological role [7–9].

EXO purification is normally based on a combination of different techniques (density gradient ultracentrifugation, size-exclusion chromatography, ultrafiltration) that successfully separate EVs according to their dimension, whereas the fractionation of EXO sub-classes of different cellular origin requires the use of affinity techniques [10–15].

Abbreviation: EV, Extracellular vesicle; VHH - Nanobody, single-domain antibody; EXO, exosomes; APO, apolipoprotein; BSA, bovine serum albumin; SEM, scanning electron microscopy; TEM, transmission electron microscopy; NTA, Nanoparticle Tracking Analysis.

* Correspondence to: Faculty of Chemistry, University of Belgrade, Department of Biochemistry, Studentski trg 16, Belgrade 11000, Serbia.
E-mail address: la_bioquimica@chem.bg.ac.rs (M. Popović).

https://doi.org/10.1016/j.nbt.2022.03.001
Received 30 September 2021; Received in revised form 11 February 2022; Accepted 6 March 2022
Available online 14 March 2022

The application of immune-based EXO capture is limited by the availability of reliable and inexpensive binders specific for biomarkers exclusively expressed on a particular EXO sub-type. Conventional antibodies have been successfully used for immune-affinity purification of EXO sub-groups [16], however they have limited applicability due to elevated production costs, genetic instability and low homogeneity after functionalization [17,18]. Finally, employing a single antibody might be necessary to discriminate among EXO sub-populations, but becomes insufficient when the most complete EXO variability sampling is necessary for downstream analyses [19]. In that case, a mix of monoclonal antibodies would be necessary and using hybridoma IgGs would further expand the costs.

Single-domain antibodies (VHH, aka nanobodies) represent a valid alternative since they are structurally stable, can be produced inexpensively in *E. coli,* are simple to engineer and label at specific residues, their clonality remains constant over the time and their short sequence allows *in silico* modelling and optimization [20–23]. Large pre-immune libraries are available and can be directly panned against soluble antigens [23–27], whole cells as well as EVs [28]. The VHHs obtained by direct panning on EVs enabled capture of vesicles from conditioned cell culture medium and human plasma [28]. Extending this approach enabled development of an affordable chromatographic matrix with anti-EV VHHs. Chromatographic matrix based on glycidyl methacrylate copolymer has already been widely used for enzyme immobilization due to the chemical versatility of its epoxy groups and the positive influence that immobilization has on protein stability and enzyme activity [29]. These copolymers seem to possess both the necessary physical and the chemical requisites [30,31] to be adapted for purification of EXOs. In this paper, a novel VHH-copolymer chromatography system was successfully used to purify EXOs from conditioned cell culture medium and human plasma.

Materials and methods

Chemicals

Polyvinylpyrrolidone (PVP, Mw = 1,300,000 g/mol), glycidyl methacrylate (GMA), ethylene glycol dimethacrylate (EGDMA), 1-dodecanol and cyclohexanol were from Sigma Aldrich (St. Louis, MO, USA). Ethylenediamine was obtained from Merck (Kenilworth, NJ, USA). Toluene and 96% ethanol were from Zorka (Šabac, Serbia). The initiator 2,2′-azobis(2-methylpropionitrile) (AIBN) (98%, Akzo Nobel, Amsterdam, Netherlands) was recrystallized twice from ethanol. Anti CD-9 Phycoerythrin (PE)-labeled (clone MM2/57), alkaline phosphatase-labeled anti-mouse IgG, cell culture media and reagents, fetal bovine serum and bovine serum albumin (BSA) were from Sigma-Aldrich (Steinheim, Germany), while anti CD-63 (clone TS63) was from Abcam (Cambridge, UK). Alexa Fluor® 488 anti-human CD63 (clone H5C6) and PE/Dazzle™ 594 anti-human CD81 (TAPA-1) antibody (clone 5A6) were from Biolegend (San Diego, CA, USA). Nitrocellulose membrane and bicinchoninic acid (BCA) Protein Quantification Kit were from Thermo Scientific (Rockford, IL, USA). Microwell plates were from Thermo Fisher Scientific (Roskilde, Denmark). All other chemicals were of analytical grade and were used without further purification.

Preparation of microporous copolymer

The diblock copolymer of glycidyl methacrylate and ethylene glycol dimethacrylate were synthesized according to the previously described procedure with some modifications [29–33].

Briefly, a continuous phase consisting of 113 mL of 1% (w/v) PVP in demineralized water was heated to 70 °C in a 250 mL reactor equipped with an anchor stirrer. A monomer phase (24.3 g of both the monomer GMA and cross-linking agent EGDMA (GMA/EGDMA = 2/3), initiator (0.25 g of AIBN) and inert phase (32.0 g, 1-tetradecanol/cyclohexanol = 4/1) were added to the continuous phase under stirring (200 rpm). The reaction was stopped after 5 h. The obtained copolymer was washed 5 times with ethanol, and dried at room temperature (RT). The particle size distribution was determined by sieve analysis and the copolymer beads with the diameter in a range from 125 to 250 μm were used for further investigation.

Diblock copolymer beads (10 g), were suspended in 250 mL of toluene. Ten-fold excess of ethylenediamine in relation to epoxy groups was added and the reaction was left to stir overnight at 25 °C. Then, the reaction mixture was first heated at 80 °C for 6 h and subsequently left stirring overnight at 25 °C. The polymer particles were removed and washed first with ethanol and subsequently with water until the pH value of the washing water was 6.0. The samples were oven-dried at 50 °C for 2 h. The concentration of amino groups was determined by elemental analysis. A scanning electron microscope (Tescan FE-SEM Mira 3 XMU) operated at 20 keV was employed to characterize the morphology of the diblock copolymer. All samples were coated with a thin gold layer using a sputter coater (Polaron SC503, Fisons Instruments) prior to the SEM analysis.

Determination of matrix pore size

The pore size distributions of the synthesized diblock copolymer beads were determined by a mercury porosimetry (Carlo Erba 2000, software Milestone 200). Mercury intrusion porosimetry measurements of the synthesized copolymers poly(GMA-co-EGDMA) were performed on a high-pressure unit PASCAL 440 (Thermo Fisher Scientific) in a CD3-P type dilatometer in the pressure range of 0.1–200 MPa. Although two consecutive intrusion-extrusion cycles were performed, the second cycle was used to calculate the porosimetric parameters, since the first cycle only provides information on the intra-particle porosity of the particles and excludes the contribution of the inter-particle voids. A SOLID Software System PC interface was used for automatic data acquisition and complete textural parameter calculations. Before analysis, the powder sample was dried by removing the supernatant and bubbling the N_2 gas for one hour, and additionally evacuating for 2 h in a sample holder at the analytical position of a Macropore Unit 120 (Carlo Erba Strumentazione) used for mercury filing of the dilatometer.

Determining static binding capacity

Binding isotherm was generated by batch experiments. Aliquots with fixed amount of polymer were incubated with increasing amounts of protein (BSA) in an equilibration buffer. Polymer was washed with an equilibration buffer (sodium phosphate buffer pH 7.0) and was then transferred to vials, each of them containing 0.25 mL of polymer. A BSA serial dilution was prepared in the same buffer and a volume of 1 mL of each of them was added to each vial. Vials were mixed gently for 48 h to achieve binding equilibrium. Protein concentration in the decanted supernatant was measured with Bradford Protein Assay. Binding capacity (mg of bound protein per mL of resin) was plotted as a function of supernatant protein concentration to create Langmuir binding isotherm. Experimental data were fitted in Langmuir adsorption model using equation $q = \frac{Qmax*c}{K_D+C}$ (Eq. 1) where Q_{max} is the equilibrium binding capacity, q and c are the respective stationary and mobile phase protein concentrations, and K_D is the equilibrium dissociation constant [34].

VHH subcloning and production

VHHs used in this work (H1, H6, D5, B1 and G2) were isolated from a naïve pre-immune library by direct panning against EVs recovered from the supernatant of cultured human cells as described previously [28]. VHH sequences were subcloned into a modified pET-14b vector between the unique *NcoI* and *NotI* sites to obtain fusion constructs of VHHs linked to eGFP and 6xHis tag at the C-terminal [35–37]. Vectors were

transformed in *E. coli* BL21(DE3) cells hosting a plasmid for the expression of sulfhydryl oxidase and DsbC [23,38,39]. VHHs were produced as previously described with some modifications [28,35]. Briefly, 3 mL of overnight pre-cultures were transferred in 400 mL of LB broth with 100 μg/mL ampicillin and 25 μg/mL chloramphenicol. Bacteria were grown at 37 ºC until they reached $OD_{600\ nm}$ 0.4. Expression of DsbC and sulfhydryl oxidase was induced by adding 0.5% (g/mL of culture) of arabinose and temperature was lowered to 30 ºC. After 30 min, 1 mM IPTG was added to induce VHH expression. The bacteria were grown overnight at 21 ºC. The next day, cells were harvested and pellet was resuspended in 20 mL of TBS buffer (50 mM Tris-HCl, 150 mM NaCl, pH 7.4). Cells were sonicated and finally centrifuged at 14,000 x *g* for 20 min at 4 ºC. Supernatant was used for IMAC chromatography. The matrix was equilibrated with buffer A (50 mM Tris, 150 mM NaCl, 15 mM imidazole pH 7.4). Unbound proteins were washed away with buffer A while bound proteins were eluted with buffer B (50 mM Tris, 150 mM NaCl, 300 mM imidazole, pH 7.4). Fractions containing VHH-eGFP were pooled and 20% glycerol was added to samples for long-term storage. Cross-reactivity with EVs from other species was not tested.

Activation and immobilization of nanobodies to polymer

Methacrylate-based copolymer was washed a few times with 0.1 M sodium phosphate buffer, pH 8.0, then incubated for 2 h at RT with 2.5% glutaraldehyde in the same buffer with occasional stirring. Excess glutaraldehyde was removed from polymer suspension by rinsing with 0.1 M sodium-phosphate buffer, pH 7.0. VHH immobilization was performed by incubating wet polymer (1 mL) with 100 μg of each of the five different VHH-GFP constructs (total of 500 μg of protein) at 4 ºC for 24–48 h with occasional shaking [31,34]. Protein concentrations before and after the reaction were determined with BCA assay and the coupling efficiency was calculated as the ratio between protein immobilized on the affinity resin and total amount of VHH used in the coupling reaction. Matrix was rinsed 3 times with 0.1 M sodium phosphate buffer pH 7.0. Free binding sites were blocked with 200 mM glycine at 4 ºC for 24–48 h with occasional shaking. Immobilized copolymer was stored at 4 ºC until further use. Stability of the VHH copolymer matrix after nanobody functionalization was tested for eight weeks.

Collection of conditioned cell-culture supernatant

Human embryonic kidney (HEK 293) cells were grown in DMEM medium supplemented with 10% FBS and 100 U/mL penicillin and 100 μg/mL streptomycin. Immortalized human T lymphocytes (Jurkat cell line) were grown in RPMI medium supplemented with 10% FBS, 100 U/mL penicillin and 100 μg/mL streptomycin. Cells were grown at 37 °C under a 5% CO_2/95% air atmosphere at constant humidity.

HEK cells were grown until a confluence of 70–80%, while Jurkat cells were grown in RPMI medium supplemented with FBS for 3 days. The cultured medium was removed and cells were washed with phosphate buffered saline (PBS) before adding either FBS-free DMEM medium (HEK) or FBS-free RPMI medium (Jurkat). Cells were grown for a further 48 h and then conditioned cells culture supernatants were collected in 50 mL polypropylene (PP) tubes. Cells were removed by centrifugation (30 min at 300 x *g* at 4 ºC). Supernatants were transferred to sterile tubes and used for chromatographic separation of EVs.

Plasma collection and processing

Blood samples from healthy control individuals (3 males, 2 females, age range 25–32) were collected after obtaining written informed consent to the study, which was approved by the Ethics Committee of University of Belgrade, Faculty of Chemistry. The collection was performed in accordance with the Declaration of Helsinki. Peripheral venous blood was collected in Vacutainer (Becton Dickinson) tubes with citrate as anticoagulant and processed within 30 min of collection. Blood was first centrifuged (30 min at 1550 x *g* at RT) to remove cells. Platelet-free plasma (PFP) was obtained by centrifugation (30 min at 3200 x *g* at RT). Aliquots of plasma were maintained at − 80 °C until use or further processed to isolate EVs. Blood from each donor was collected 3 times during a six month period, at two months interval.

Purification of EV-enriched fractions from conditioned cell culture media and human plasma using immunoaffinity chromatography

The VHH-activated copolymer (0.5 mL) was blocked with 5% (w/v) skimmed milk in PBS for 30 min at RT to block any remaining active sites on the copolymer surface. Then it was washed extensively with PBS and incubated with: (a) 500 μL of plasma pooled from healthy donors (group of 5 volunteers), diluted 1:2 in PBS with 1% milk; (b) 30 mL of conditioned cell culture medium from HEK or Jurkat cells diluted 1:2 in the same buffer for 1 h at RT. The copolymer was transferred into an empty gravity column (PP, inner diameter 6.5 mm, height 62 mm). Unbound proteins were washed away with PBS and bound vesicles were eluted in 425 μL of 200 mM glycine, pH 2.2 and collected in PP-tubes pre-filled with 75 μL of neutralization buffer (1 M Tris-HCl pH 9.0). The elution step was repeated until the Bradford assay indicated that no further protein was eluted. Concentration of proteins in eluted fractions was determined using Bradford assay.

Determination of EXO protein and lipid content

The amount of protein collected in chromatographic fractions was determined with Bradford reagent using BSA as a standard.

Total lipid determination of EXO preparations was determined using the colorimetric sulfophosphovanilin (SPV) assay [40]. The solutions of lipid standards were prepared with cholesterol in chloroform. Fifty μL of EXO preparations were extracted with 70 μL of chloroform. The chloroform was then evaporated in a heat block by incubating the tubes at 90 °C for 10 min. Fifty μL of PBS were added to each dried sample and to each tube containing the lipid standards. Then, 250 μL of 96% sulphuric acid were added to the tubes followed by incubation with open lids at 90 °C for 20 min in a heat block. An aliquot of 220 μL of each sample/standard was transferred into a 96-well polystyrene plate and allowed to cool to RT. Finally, 110 μL of 0.2 mg/mL vanillin in 17% phosphoric acid were added to each well, the plate was incubated for 10 min at RT and sample absorbance was measured at 540 nm [41]. Lipid concentration of EV samples was expressed as cholesterol concentration.

EXO quantification and morphology

EXO particle size distribution and number was determined on a NanoSight LM10 system (Malvern Preanalytical, Malvern, UK) by analysing ~500 μL of affinity chromatography-isolated EV preparations diluted in PBS (~10^3–10^4 times). Individual videos of 60 s for each sample were acquired using the maximum camera gain and analysed by the NanoSight particle tracking software to determine particle size and density.

Morphology of eluted vesicles was evaluated by transmission electron microscopy (TEM) after sample negative staining. The EXO suspension was applied to carbon coated grids. After EXO adsorption, the excess of suspension was removed and each grid was fixed in 2.5% glutaraldehyde. EXOs were further contrasted by 1% phosphotungstic acid and allowed to air dry. Electron micrographs were collected using a Philips CM12 electron microscope (Philips, Eindhoven, The Netherlands) equipped with the digital camera SIS MegaView III (Olympus Soft Imaging Solutions, Münster, Germany).

EXO morphology was also analyzed using scanning electron microscopy (SEM). The EXO suspension was fixed with 2.5% glutaraldehyde in PBS for 10 min at RT. Samples were then loaded onto metal stubs and

air dried. A scanning electron microscope,Tescan FE-SEM Mira 3 XMU (Tescan, Brno, Czech Republic), operated at 20 keV was employed to characterize the EV morphology. All samples were coated with a thin gold layer using a sputter coater (Polaron SC503, Fisons Instruments) prior to SEM analysis.

EXO marker analysis

EXO samples isolated from cell culture supernatants and human plasma (40 µL corresponding to 200 µg protein) were mixed with 10 µL of buffer for sample preparation (5 x stock solution: 60 mM Tris buffer pH 6.8, 30% glycerol, 10% SDS, 2-Mercaptoethanol, 1% Bromophenol Blue and deionized water). Samples were heated at 95 ºC for 5 min and then loaded onto polyacrylamide (4% stacking and 14% resolving) gel. Sodium dodecyl sulfate – polyacrylamide gel electrophoresis (SDS-PAGE) was run under reducing conditions at 190 V for 1 h [42]. Then proteins were transferred to a nitrocellulose membrane for 45 min, at 55 mA. After blocking with Tween-Tris Buffered Saline (tTBS, 0.1% Tween-20, 20 mM Tris, 0,9% NaCl, pH 7.4) containing 1% of skimmed milk for 1 h at RT, proteins were incubated with primary antibodies (diluted 1:3000 in TBS with 0.1% BSA). Alkaline phosphatase-labeled anti-mouse IgG secondary antibodies (dilution 1:1000) were used for visualization in the presence of 5-bromo-4-chloro-3-indolyl phosphate (BCIP)/4-nitroblue tetrazolium (NBT) (Sigma–Aldrich, Germany).

Flow-cytometry was performed by coating aldehyde/sulfate latex beads (4% w/v, 4 µm; Sigma-Aldrich) with EVs. Thirty µL beads were coated overnight at 4 ºC with 40 µg of total protein from EV-enriched fractions in PBS. Beads were washed 3 times with PBS and blocked first for 30 min at RT with 200 mM glycine and then 30 min in PBS plus 5% (w/v) skimmed milk. Beads were washed 3 times in PBS before adding anti-CD9 antibodies (dilution 1:5) and incubated 1 h at 37 ºC. When anti-CD-63 (dilution 1:5) and anti CD-81 (dilution 1:5) antibodies were used for detection, beads were incubated for 1 h at RT. After washing, beads were analyzed using a BD FACSCalibur (BD Biosciences) collecting around 1000 events/s. A blue solid state 200 mW laser at 488 nm was used for excitation. The emission was detected at 525 nm (FL1, AlexaFluor 488), 561 nm (FL2, PE) and 620 nm (FL3/PE/Dazzle 594). The positive beads were gated on the FL1-AlexaFluor 488, SSC plot, FL2-PE, SSC plot and FL3-PE/Dazzle 594, SSC plot. AlexaFluor 488, PE and/or PE/Dazzle 594 specific fluorescence was assessed as the signal increase with respect to negative control (autofluorescence of beads not coated with EVs, blocked with milk and incubated with antibodies).

Detection of lipoprotein contaminants

Apolipoprotein A1 (APO-A1) and Apolipoprotein B (APO-B) were detected in a commercial clinical laboratory using immunoturbidimetric test by Abbott Laboratories on Alinity ci Analyzer (Abbott Laboratories, USA). Tests were performed according to the manufacturer's instructions.

Statistical analysis

Statistical analysis was performed using GraphPad Prism v7 for Windows (GraphPad Software, San Diego, CA, USAa). A significance level of $p \leq 0.05$ was used for analysis of variance, implemented using the Kruskal–Wallis test followed by the Tukey's post hoc test ($p \leq 0.05$). Correlation between different parameters was performed at significance level of $p \leq 0.05$.

Results

Polymer synthesis and characterization

Polymer particle size was evaluated as being in the range of 125 – 250 µm while particle surfaces appeared highly porous (Fig. 1A). Modal pore diameter of copolymer after blocking and functionalization was determined to be above 90 nm (Supplementary Table 1), namely smaller than the values (150 nm) reported in the literature [43]. The conversion of the amination reaction was determined by the elemental analysis. The concentration of 0.0259 g of amino groups per 1 g copolymer was determined.

Static binding capacity of the copolymer matrix was quantified using BSA as a model protein. Langmuir binding isotherms were obtained after fitting the amount of protein bound per unit of resin volume plotted as the function of the unbound protein concentration and into Eq. Eluate pools from replicate runs ($n = 2$) were sampled and analysed.

The equilibrium binding isotherm after 48 h incubation is presented in Fig. 1B. The binding isotherm is nearly rectangular while the static or equilibrium binding capacity Q_{max} was 48.10 mg/mL. The equilibrium dissociation constant K_D was in the range of 2.62 nM indicating a strong binding interaction and high matrix capacity of synthesized co-polymer.

VHH-eGFP immobilization and stability on copolymer

The VHH-eGFP constructs used bind to unknown, probably multiple EV biomarkers and have been expressed and purified by immobilized metal affinity chromatography (IMAC), as previously described [28]. Antibody yields were in the range of 3–5 mg/L of cell culture medium. Homogeneity of purified VHHs was determined using SDS-PAGE (data not shown).

100 µg of each VHH-eGFP was immobilized covalently onto 1 g of dry aminated copolymer by means of glutaraldehyde linkers. The VHH immobilization efficiency was estimated at $> 99\%$, as no remaining protein was detected in the unbound fraction using the BCA method. Stability of each VHH-eGFP construct was assessed during an 8 week period of storage at 4 °C by quantifying the binding capacity of the activated resin. Aliquots of VHH-copolymer were taken weekly and used to purify EVs from plasma of healthy donors. The protein concentration in the resulting samples was determined and compared (Fig. 2A). There was no significant difference between the constructs in terms of loss of functionality, since all showed complete stability during the first 4 weeks of storage and a similar decline (20–25%) starting from week 6. Specifically, the binding capacity at the 8th week decreased by: 26.2% ± 1.36% (H1); 23.3% ± 0.97% (H6); 27.1% ± 1.73% (D5); 25.8% ± 1.08% (G2); and 25.9% ± 1.48% (B1). There was no statistically significant difference among the five constructs. EVs isolated from each time point were further tested by flow cytometry and all resulted positive for the CD9 biomarker (Fig. 2B).

Isolation of EXOs on VHH-copolymer

One g of copolymer was functionalized with 100 µg of each of the five VHHs to obtain a total of 500 µg of VHH per g of copolymer and the polyclonal matrix was used for EV purification from diluted, unfractionated conditioned cell culture medium and human plasma from healthy donors. Binding was performed in batch with gentle agitation after which the matrix was packed in a column and washed thoroughly with PBS. Bound material was eluted in acidic buffer and the corresponding protein chromatograms were recorded (Fig. 3). One elution peak was observed when conditioned cell-culture media were used (Fig. 3A), and tested positive for EXO biomarkers in flow cytometry (Fig. 4). A major peak with shoulders resulted from the elution of EVs from human plasma (Fig. 3B) and in this case the material was also positive for EXO biomarker (Fig. 4). The blocking agent (milk) did not contain detectable EVs and did not affect the results of chromatography (Supplementary Figs. 1 and 2).

A clear shift in fluorescence signal resulted as the consequence of the addition of the anti-CD9 PE antibody (Fig. 4A) to vesicles obtained from conditioned medium from HEK and Jurkat cells as well as from the plasma pool (30.20 ± 1.42%; 28.35 ± 2.62% and 24.05 ± 5.44%,

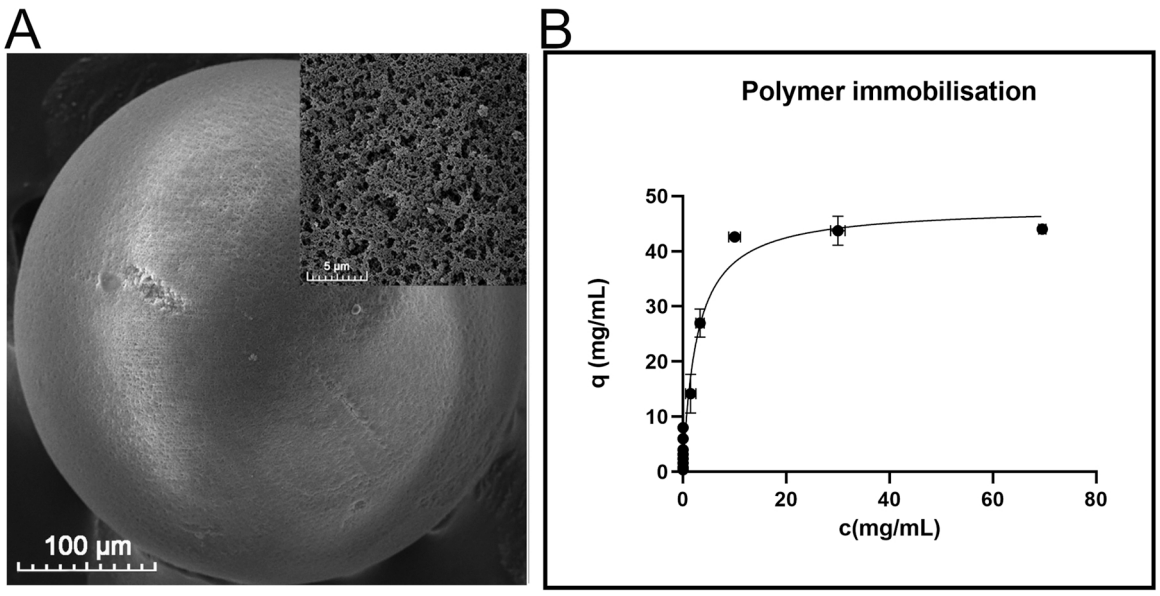

Fig. 1. Characterization of polymetacrylate co-polymer matrix: A) Scanning electron microscopy image of methacrylate co-polymer under different magnification: the round structure of the matrix can be seen at magnification of 500x; highly porous nature of the co-polymer is visible at magnification of 10,000x (upper right corner) B) The adsorption isotherm plots for BSA: Static binding capacity of the copolymer matrix was quantified using BSA as a model protein. Langmuir binding isotherms were obtained after fitting the amount of protein bound per unit of resin volume (c; mg of adsorbed protein per mL of resin) plotted as the function of the unbound protein concentration after 48 h of incubation (q; mg/mL).

respectively). Similarly, a shift in fluorescence was observed in all the tested samples when anti CD63 (Fig. 4B) and anti CD81 (Fig. 4C) antibodies were added to EXOs from media or plasma (CD63: 30.95 ± 0.78% HEK; 20.20 ± 0.57%; Jurkat; 13.90 ± 0.14% for plasma; CD81: 26.65 ± 0.50% HEK; 19.45 ± 0.21%; Jurkat;13.45 ± 070% plasma pool).

The presence of CD63 was confirmed by western blot as well (Fig. 4 D, E) that enabled identification of a band of the expected molecular weight (approximately 50 kDa) in EXO samples obtained from both Jurkat cell medium (Fig. 4D) and human plasma (Fig. 4E).

Number and morphology of isolated EXOs

Qualitative analysis of isolated EXOs was performed using the TEM and SEM analysis (Fig. 5). TEM micrographs demonstrated that the isolated EVs have a cup-like shape in the range of 50–200 nm (Fig. 5A). Size and morphology of isolated EXOs was further confirmed by SEM. As shown in Fig. 5B, C, isolated EXOs were spherical and ranged in size from 50 nm to 200 nm.

Nanoparticle tracking analysis was used to determine size and number of isolated EXOs (Fig. 6). Mean particle size for HEK derived EXOs was 164.0 ± 64.7 nm (Fig. 6A, E). However, particles were grouped into two major population peaks of 156 and 216 nm (Fig. 6A). Similarly, for Jurkat derived EXOs, the mean particle size was 147.2 ± 55.4 nm, with four major populations of 52, 103, 149, 223 nm (Fig. 6B,E). Plasma derived EXOs had a mean particle size of 195.4 ± 88.3 nm, having two different size populations of 152 and 234 nm (Fig. 6C, E). There was no significant difference in the mean particle size of analyzed EXOs. Samples used for NTA were normalized by protein concentration to approximate the particle number in HEK-derived EVs ($4.01 \times 10^9 \pm 0.01 \times 10^9$ particles/mL) and in Jurkat EVs $2.01 \times 10^9 \pm 0.03 \times 10^9$ particles/mL and $4.05 \times 10^9 \pm 0.01 \times 10^9$ particles/mL, respectively (Fig. 6D, Table 1).

Reproducibility and purity of EV fractions

The reproducibility of the chromatographic EV purification method was investigated using a plasma pool from five healthy volunteers collected at three different time points (Fig. 7). The mean amount of protein isolated from 1 mL was 0.11 ± 0.01 mg while the amount of lipids was 3.94 ± 0.92 mg. Flow cytometry confirmed the presence of the CD9 marker in the different eluate samples (Fig. 7A). There was no statistically significant difference in the amount of isolated protein (Fig. 7B), or lipid (Fig. 7C).

APO-A1 is the marker protein for HDL, while APO-B can be found on VLDL, IDL, and LDL. Plasma samples used for purification of EXOs had values of APO-A1 and APO-B 109.5 ± 2.3 mg/dL and 79.5 ± 1.4 mg/dL, respectively. Although EXOs isolated from plasma were concentrated 10-fold, both APO-A1 and APO-B were below the limits of detection of 7 mg/dL and 5 mg/dL, respectively.

Discussion

EVs released by all cell types are present in biological fluids and, since their composition and content mirror that of the parent cells, they are considered useful biomarkers for assessing physiological and especially pathological conditions [44–46]. Recent studies demonstrate that EXOs have a role in many diverse biological processes ranging from apoptosis, coagulation, antigen-presentation, cell homeostasis, inflammation, intrecellular signalling, angiogenesis, and growth and metastasis of tumors [4].

Various biophysical and biochemical properties can be used to isolate EVs, including dimension, density, shape, surface charge and antigen display [47]. At the end of 2015, differential ultracentrifugation was the most commonly used method for EV separation (81% of studies), according to a worldwide ISEV survey [48]. Other techniques including density gradients, precipitation, filtration, size exclusion chromatography and immuno-isolation are also used for that purpose. Most reports combine one or more methods to achieve better results in the case of subtype separation or to increase the specificity of separated EVs, but the level of contaminants such as albumin, immunoglobulins and lipoproteins can remain elevated [19]. Despite collective efforts, there is no standardized method for isolating and purifying specific subtypes of circulating EVs from human plasma.

Immunoaffinity based methods could offer a reliable approach for EXO isolation, especially in the cases of pathological conditions [19].

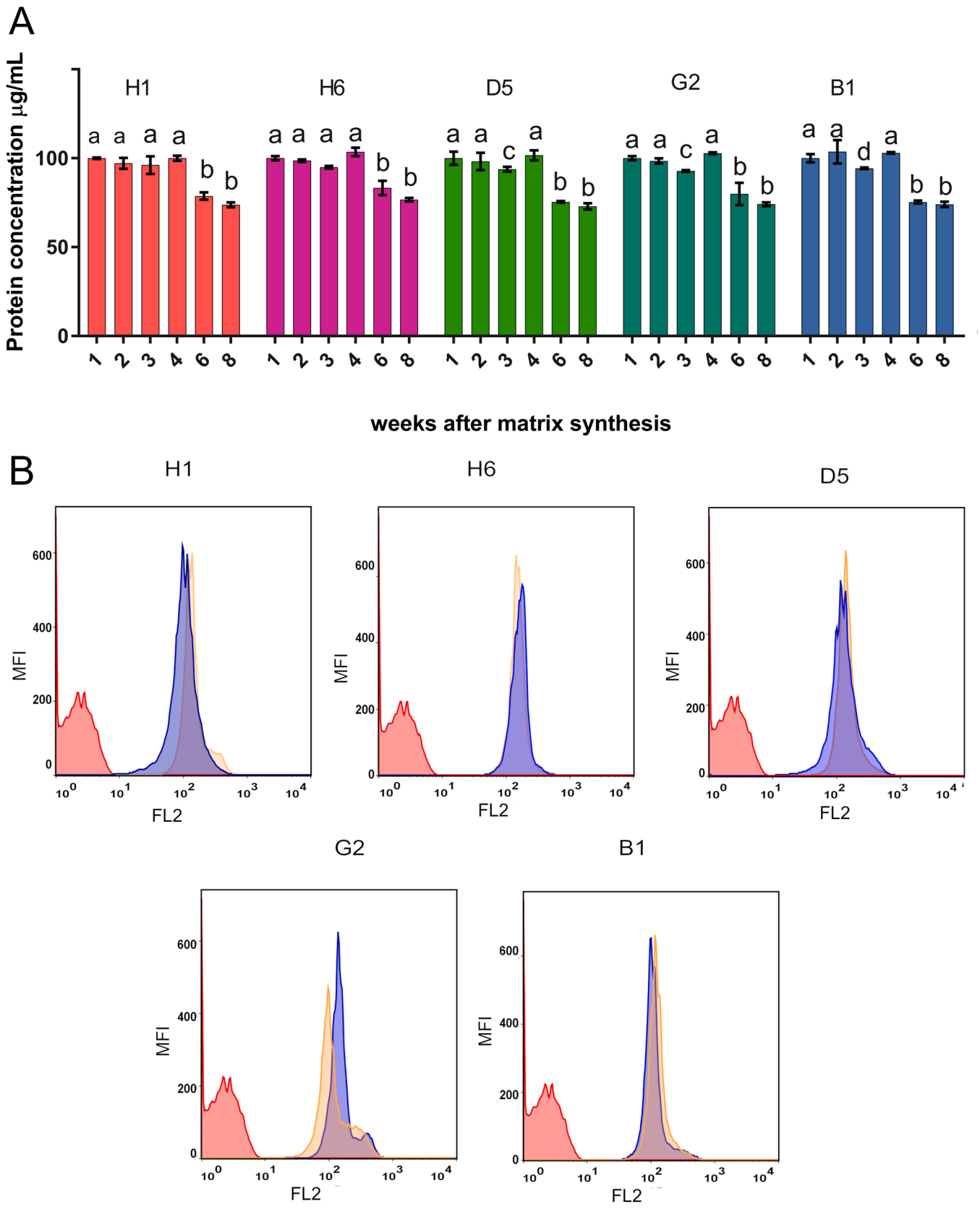

Fig. 2. Determination of stability of VHH on co-polymer resin. Individual VHHs were produced and immobilized on methacrylate co-polymer. Synthesized matrix was stored in PBS at 4 °C for 8 weeks and aliquots were taken at different time points to determine storage stability. Chromatography was performed using human plasma as source of EXOs. EXO isolates at different time points were analysed for A) concentration of protein; B) presence of CD9 marker. Gates were set according to the values of autofluorescence of naked beads (not coated with EVs; blocked with glycine and milk; red line). Presence of EVs was detected by measuring the binding of anti-CD9 PE at week 1 (blue line) and week 8 (orange line). H1, H6, D5, G2, and B1 represent isolates from VHH-matrices synthesized with respective VHH. The error bars indicate standard deviations for triplicate measurements. Means with different letters are significantly different (Tukey's HSD, $p \leq 0.05$).

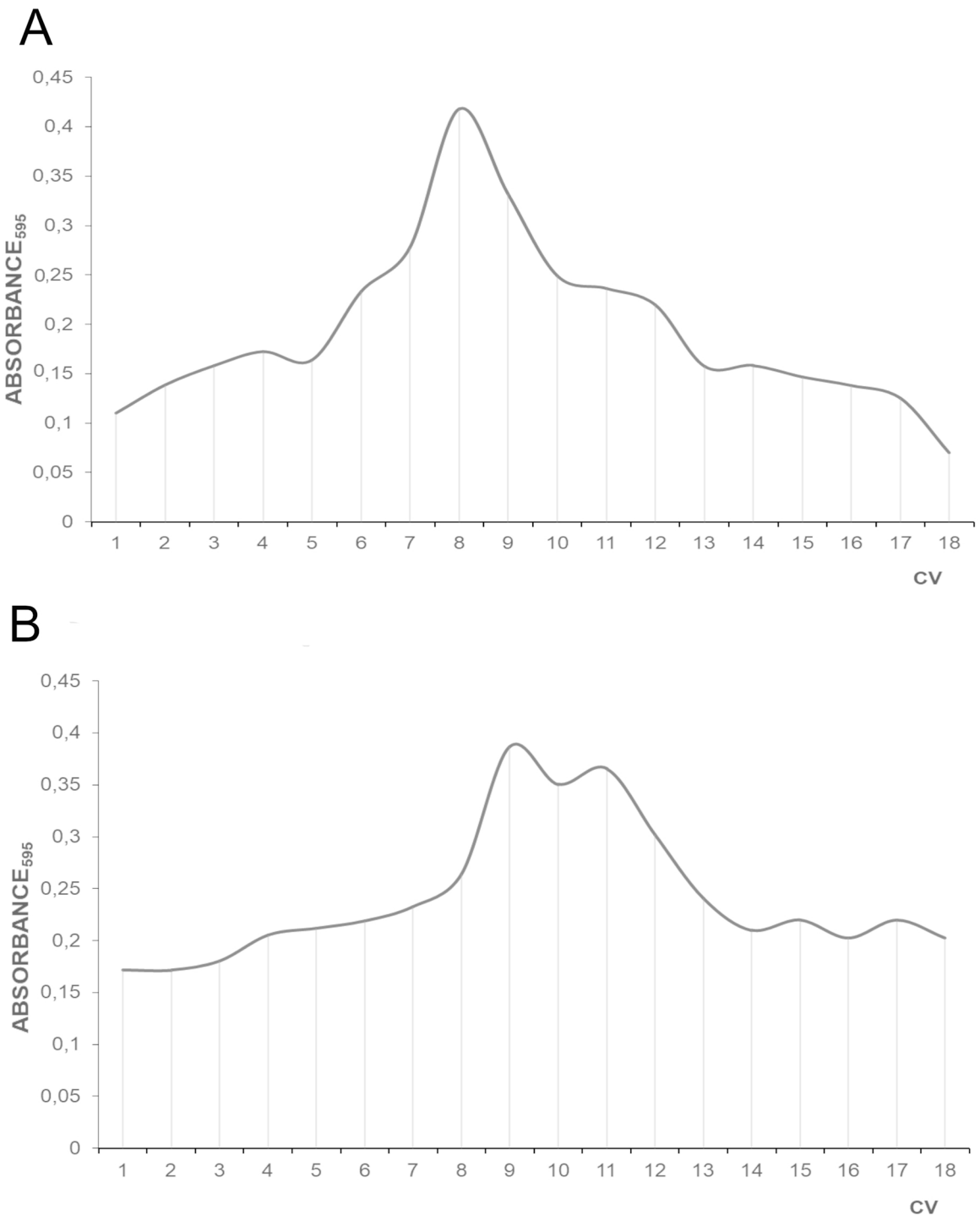

Fig. 3. Chromatographic separation of EV-containing fractions present in cell culture media and human plasma pool. EVs present in cell culture supernatant (A) and pool of plasma from healthy volunteers (B) were separated using an immunoaffinity resin composed of five different VHH constructs immobilized on polymethacrylate co-polymer.

Specific antigens such as members of the human epidermal growth factor receptor (EGFR) family [49] EpCAM, Mart-1, or TYRP2 are selectively displayed on the outer surface of EXOs generated by different tumors. Nonetheless at the present, immunoaffinity approaches have mostly exploited antibodies against universal EXO biomarkers such as CD63 for the terminal purification step [50–53]. The introduction of protocols exploiting new antigen/antibody pairs for the isolation of exclusive EXO subtypes is therefore particularly intriguing. However, immunoaffinity is usually coupled to a biosensor surface or (magnetic) beads that enable the recovery of minimal amounts of EXO sufficient for diagnostics but not for more accurate biological analysis that could be possible with a scalable and affordable method of EXO purification.

In this study the efficiency of immunoaffinity for the capture and purification of EXOs from biological fluids of varying complexity using VHH-activated methacrylate-based copolymer was evaluated. Methacrylate based copolymer has traditionally been used for enzyme immobilization due to its stabilizing effect [31,33,54] and, in the absence of capturing VHHs, was inert towards EV and any protein present in

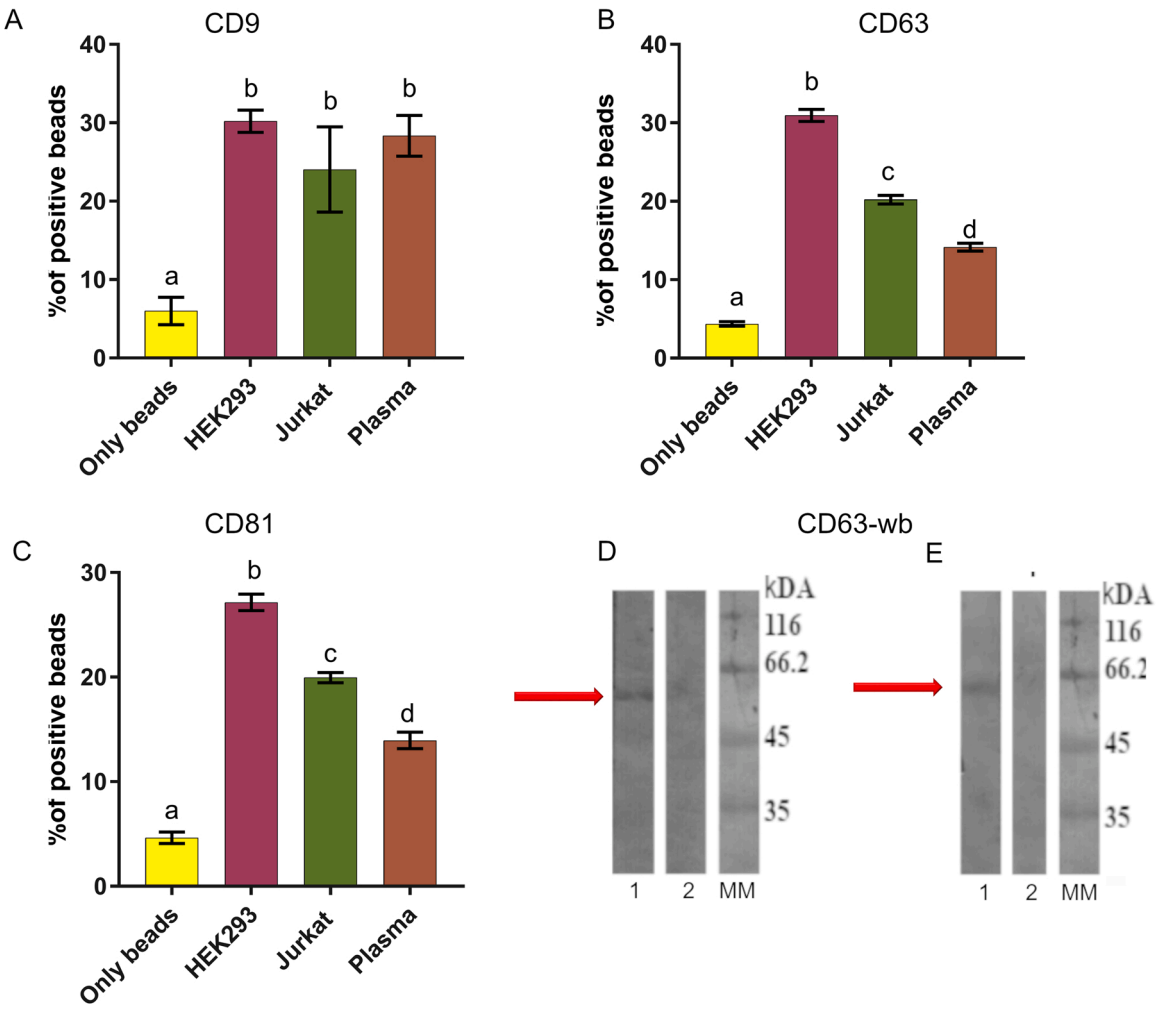

Fig. 4. Detection of EV surface markers in isolates from cell culture supernatant and human plasma detected by flow cytometry and western blot. Isolated EXOs were immobilized on latex beads, which were than treated with glycine and milk for blocking, after which the surface markers were detected by flow cytometry using A) Anti CD9-PE, B) Anti-CD63-AlexaFluor488 and C) Anti-CD81 PE/Dazzle. Latex beads without EXOs treated with glycine and milk were used as a control. CD63 was detected in western blot (annotated with red arrow) from D) cell culture supernatant and E) human plasma. Lane 1 represents the sample, while lane 2 is the control of secondary antibody. The error bars indicate standard deviations for triplicate measurements. Means with different letters are significantly different (Tukey's HSD, $p \leq 0.05$).

biological samples (Supplementary Fig. 2). It formed pores of dimensions theoretically compatible with the size of only the smallest EXO fraction and, since a further significant reduction in mean pore diameter was induced by VHH immobilization and surface blocking, it is probable that most of the interactions between EVs and VHHs occurred on the matrix surface. VHH-GFP nanobodies were attached covalently to such matrix by using glutaraldehyde as linker. Although the Qmax was not determined for each individual VHH, the maximal amount of BSA bound per 1 mL was 48.1 mg or 723.6 μM of protein. VHHs were coupled well below this limit, approximately 7.1 μM of each individual nanobody or 35.8 μM in total, a concentration significantly below the theoretical limit to minimize steric hindrance between VHH-immobilized EXOs. Low amounts of nanobodies for matrix functionalization were used to avoid activity loss as well as EV competition for active sites on the capture surface [55]. Coupling efficiency under given conditions was > 99% as no protein was detected in the removed buffer after coupling. This innovative chromatographic matrix was effectively used to purify EXO and when preserved at 4 °C in PBS its functionality was stable for 4 weeks, a period after which a loss of VHH activity in the absence of stabilizing agents can be expected [56,57].

VHH construct immobilization on the matrix involved the protein primary amine groups, a random process that might lead to loss of binding capacity if part of the paratopes became inaccessible to the antigens [55]. To minimize such an effect, VHHs fused to eGFP were used as immunocapture elements. Binding the VHH-eGFP chimeric molecules to the surface of methacrylate-based copolymer increases the chance of proper orientation as the eGFP portion of the molecule harbors 17 Lys residues, compared to only two present in the VHH scaffold. In such a set-up statistically only about 10% of the VHHs should be blocked in a probably unproductive conformation.

Immunoaffinity capture has already been found to be superior to ultracentrifugation and density gradient separation as it was able to enrich EXO markers, and EXO-associated proteins by at least twofold more than the other two methods studied [10]. Recombinant antibodies can be selected from immune or naïve libraries. Immune libraries usually provide high affinity binders but, depending on the antigen, diversity is sometimes limited. On the other hand, non-immune (naïve) libraries, from which the binders used in this work derived, provide a higher diversity of binders, but high affinity can be reached only when selecting from very large functional libraries [25]. VHH nanobodies used in this work were selected from a naïve library and have already demonstrated a stabilizing effect on EXOs during immunocapture on solid surfaces and their differing binding characteristics suggest that they recognize different epitopes [28]. Using a blind approach in VHH

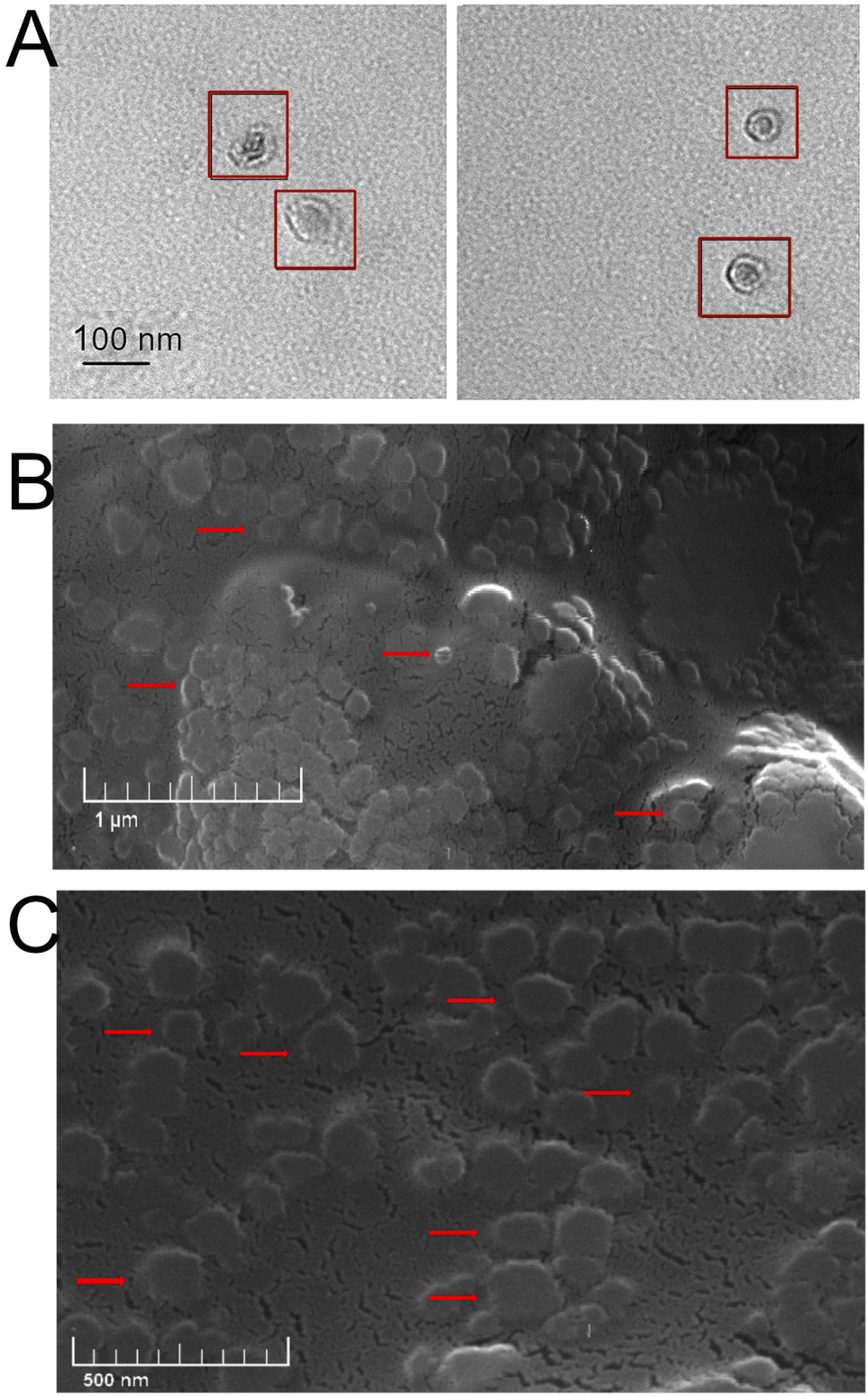

Fig. 5. TEM (A) and SEM (B, C) analysis of immuno-purified EXOs. EXOs recovered from human plasma were analysed by: A) TEM after PTA negative staining at a magnification of 40,000x; B) SEM after gold staining under magnification of 50 000x and C) SEM after gold staining at a magnification of 100,000x. The image shows the EV dimension variability (50–200 nm). Red boxes and red arrows denote EVs of different dimensions.

isolation allowed the isolation of binders with distinct binding features in terms of specificity and affinity, but made it difficult to determine their respective antigen targets as well as their affinities [28].

One of the main disadvantages of immunoaffinity capture lies in the fact that using particular antibodies may select for some sub-sets of vesicles present and in that sense insufficiently reflect the complexity of the original sample [19]. By using a combination of five different VHH constructs with different specificities it was aimed to generate a poly-clonal matrix with a wider binding range towards EXOs and probably synergistic capacity. Two major parameters are likely controlling the

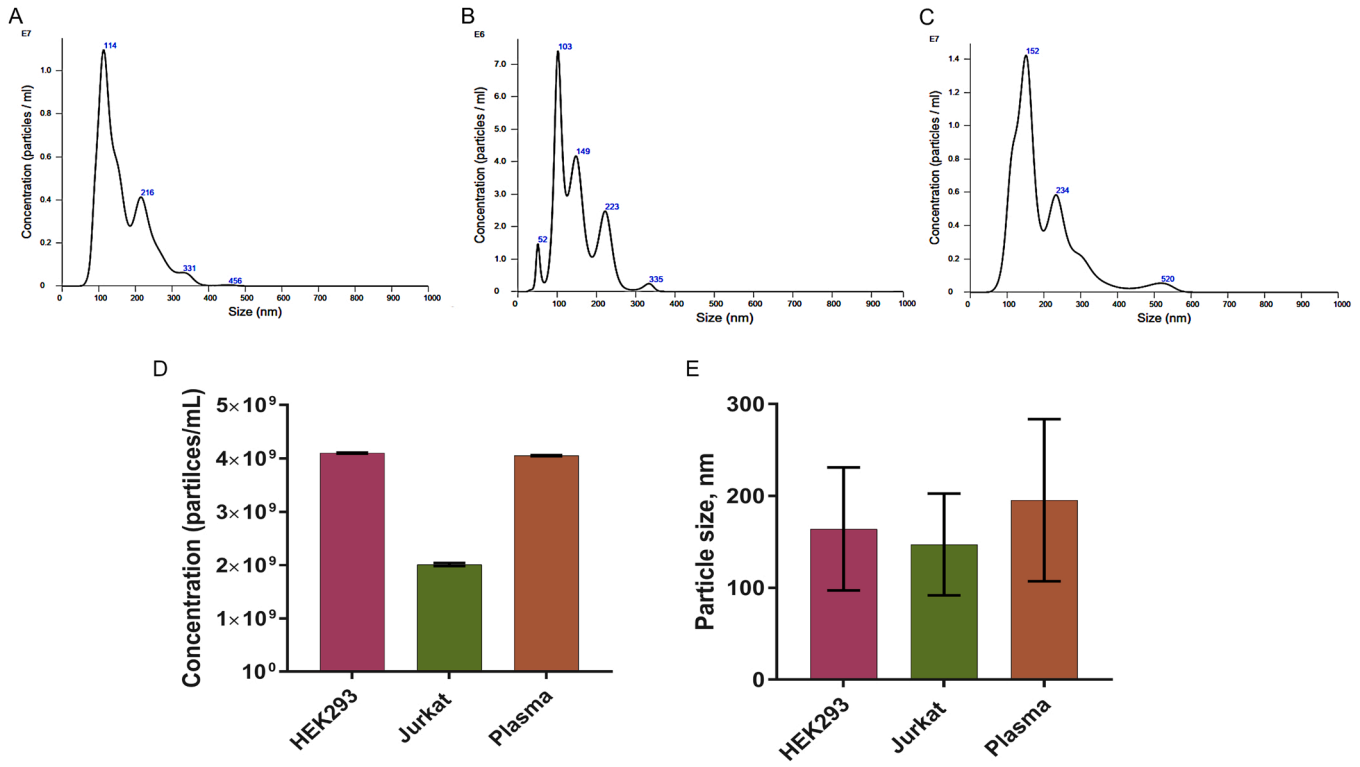

Fig. 6. Characterization of EVs using nanoparticle tracking analysis (NTA). Representative size distribution profiles of EVs isolated from (A) HEK cell culture supernatant, (B) Jurkat cell culture supernatant and (C) human plasma. NTA was used to determine (D) concentration of particles/mL and (E) median size (nm) of isolated EV samples.

Table 1
Summary of characteristics of EXO isolated using VHH GFP polymethacrylate co-polymer affinity resin: SEM-Scanning electron microscopy; TEM-transmission electron microscopy; ND-Not determined.

Sample	HEK293	Jurkat	Plasma
Starting volume, mL	25	25	0.5
Final protein concentration, mg	0.17 ± 0.02	0.37 ± 0.03	0.11 ± 0.01
Tetraspanin detection	CD9 + / CD63 + / CD81 +	CD9 + / CD63 + / CD81 +	CD9 + / CD63 + / CD81 +
Apolipoptotein detection	ND	ND	ApoA1-/ApoB-
Mean particle size, nm	164.0 ± 64.7	147.2 ± 55.4	195.4 ± 88.3
Particle concentration x 10^9	4.01 × 10^9 ± 0.01	2.01 × 10^9 ± 0.03	4.05 × 10^9 ± 0.01
SEM	ND	ND	Single vesicles, 50–200 nm
TEM	ND	ND	Single vesicles, 50–200 nm

binding kinetics between an immune-activated matrix and EXOs in solution, namely the affinity of the VHHs and the avidity effect dependent on the VHH density on the surfaces. Even though these parameters remain unknown, binders selected from pre-immune libraries have generally moderate affinity toward the antigen [58]. Whereas high affinity antibodies can make release of EVs difficult, consequently damaging their integrity [59], it seems that the combination of moderate binder affinity and low density of active VHHs on the matrix used in the present experiments resulted in a chromatographic matrix with "optimal" conditions, namely functional enough to capture the vesicles but enabling their release under relatively mild conditions. EXOs' native biological features were confirmed by the presence of tetraspanin biomarkers (Fig. 4) and morphological integrity (Figs. 5 and 6).

Yield and purity of isolated EV varies significantly between methods and usually a lower yield is attributed to samples of greater purity [60]. The particle concentration reported in this work is similar to that which could be obtained by ultracentrifugation, but the low total protein content suggests fewer contaminants in our samples [60]. Furthermore, no lipoprotein biomarkers APO-A1 and APO-B were detected in the purified EXOs.

Conclusion

In this work, the first report on the use of spherical porous methacrylate-based copolymer coupled with VHH antibodies for isolation of EVs from biological fluids was described. This inexpensive and simple immunoaffinity method was successfully applied for the isolation of vesicles that have the morphological and biochemical characteristics of EXO.

Funding

This work was funded by Ministry of Education, Science and Technological Development of Republic of Serbia Contract number: 451-03-68/2022-14/200168 and 451-03-68/2022-14/200288 and CEEPUS Network: Advanced Trends in Education and Research of Biochemistry, Biophysics and Biotechnology of Macromolecules – CIII-RS-1310-02-1920.

Author contribution

Lidija Filipović produced the clones, isolated vesicles, performed FACS experiments and WB. **Milica Spasojević** synthesized and characterized polymer matrix. **Aleksandra Korać** performed TEM experiments. **Milica Popović** designed the project. **Milica Popović** and **Ario de Marco** conceived the experiments and wrote the manuscript, **Suzana**

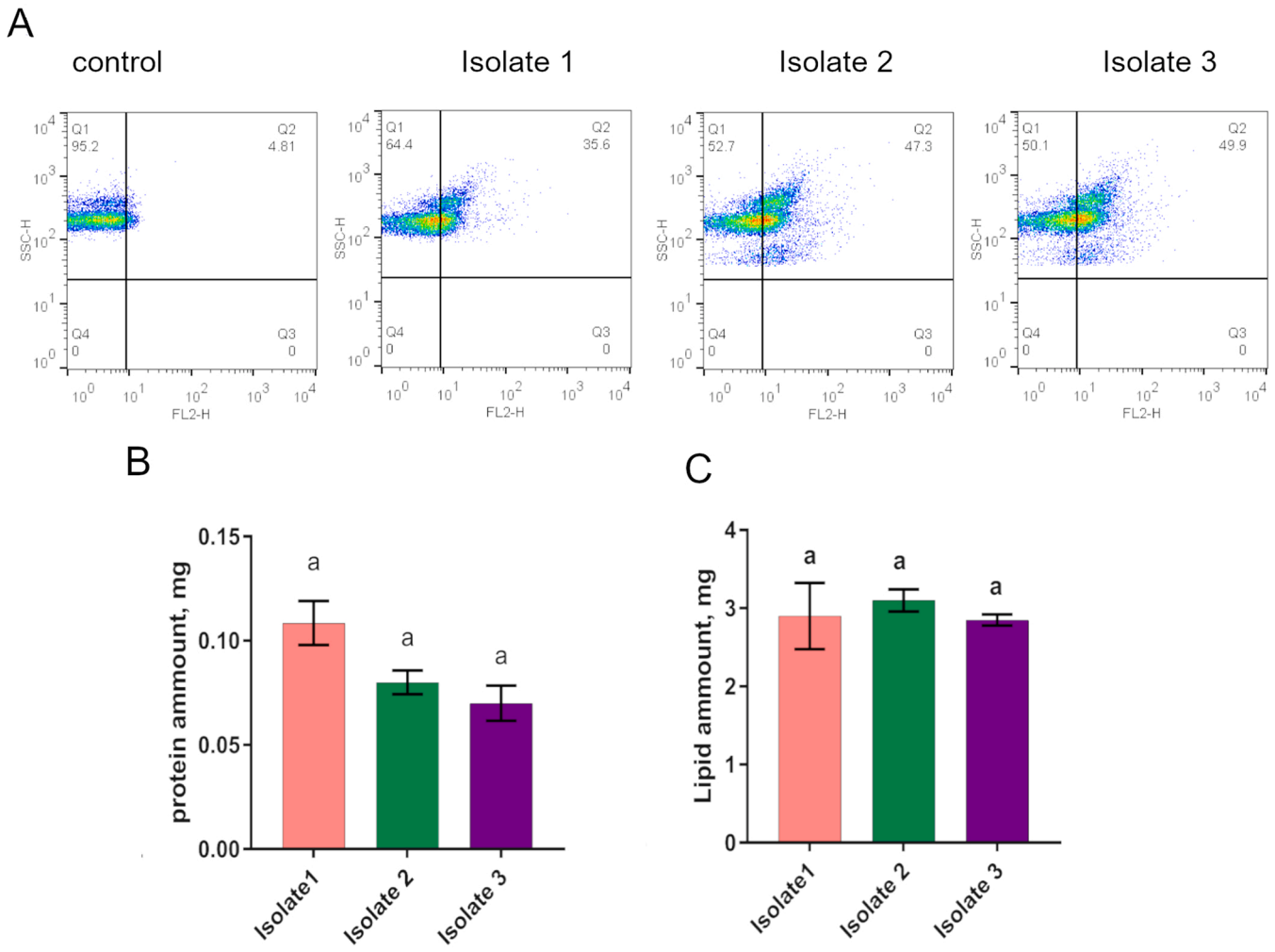

Fig. 7. Reproducibility of isolation using VHH-copolymer. Plasma pool from healthy volunteers collected at three different timepoints was subjected to EV isolation. Isolates were tested by flow cytometry in order to detect CD9 (A), while concentrations of protein (B) and lipids (C) was also detected. The error bars indicate standard deviations for triplicate measurements. Means with different letters are significantly different (Tukey's HSD, $p \leq 0.0$.

Matijaševic, **Radivoje Prodanović** and **Goran Brajušković** reviewed and edited manuscript draft. All authors read and approved the final manuscript.

Data Availability

Data will be made available on request.

Acknowledgement

The authors would like to thank Vukašin Ugrinović (SEM images) and Jugoslav Krstić (matrix porosity) for their technical assistance.

Declaration of competing interest

The authors report no declarations of interest.

Appendix A. Supporting information

Supplementary data associated with this article can be found in the online version at doi:10.1016/j.nbt.2022.03.001.

References

[1] Tschuschke M, Kocherova I, Bryja A, Mozdziak P, Angelova Volponi A, Janowicz K, et al. Inclusion biogenesis, methods of isolation and clinical application of human cellular exosomes. J Clin Med 2020;9:436. https://doi.org/10.3390/jcm9020436.
[2] Hessvik NP, Llorente A. Current knowledge on exosome biogenesis and release. Cell Mol Life Sci 2018;75:193–208. https://doi.org/10.1007/s00018-017-2595-9.
[3] Raposo G, Nijman HW, Stoorvogel W, Liejendekker R, Harding CV, Melief CJ, et al. B lymphocytes secrete antigen-presenting vesicles. J Exp Med 1996;183:1161–72. https://doi.org/10.1084/jem.183.3.1161.
[4] der Pol E, Böing AN, Harrison P, Sturk A, Nieuwland R. Classification, functions, and clinical relevance of extracellular vesicles. Pharmacol Rev 2012;64:676–705. https://doi.org/10.1124/pr.112.005983.
[5] Zhou B, Xu K, Zheng X, Chen T, Wang J, Song Y, et al. Application of exosomes as liquid biopsy in clinical diagnosis. Signal Transduct Target Ther 2020;5:144. https://doi.org/10.1038/s41392-020-00258-9.
[6] Yamashita T, Takahashi Y, Takakura Y. Possibility of exosome-based therapeutics and challenges in production of exosomes eligible for therapeutic application. Biol Pharm Bull 2018;41:835–42. https://doi.org/10.1248/bpb.b18-00133.
[7] Escrevente C, Keller S, Altevogt P, Costa J. Interaction and uptake of exosomes by ovarian cancer cells. BMC Cancer 2011;11:108. https://doi.org/10.1186/1471-2407-11-108.
[8] Gonzales PA, Pisitkun T, Hoffert JD, Tchapyjnikov D, Star RA, Kleta R, et al. Large-scale proteomics and phosphoproteomics of urinary exosomes. J Am Soc Nephrol 2009;20:363–79. https://doi.org/10.1681/ASN.2008040406.
[9] Jeppesen DK, Nawrocki A, Jensen SG, Thorsen K, Whitehead B, Howard KA, et al. Quantitative proteomics of fractionated membrane and lumen exosome proteins from isogenic metastatic and nonmetastatic bladder cancer cells reveal differential expression of EMT factors. Proteomics 2014;14:699–712. https://doi.org/10.1002/pmic.201300452.
[10] Tauro BJ, Greening DW, Mathias RA, Ji H, Mathivanan S, Scott AM, et al. Comparison of ultracentrifugation, density gradient separation, and

immunoaffinity capture methods for isolating human colon cancer cell line LIM1863-derived exosomes. Methods 2012;56:293–304. https://doi.org/10.1016/j.ymeth.2012.01.002.
[11] Taylor DD, Gercel-Taylor C. Exosomes/microvesicles: mediators of cancer-associated immunosuppressive microenvironments. Semin Immunopathol 2011; 33:441–54. https://doi.org/10.1007/s00281-010-0234-8.
[12] Ghosh A, Davey M, Chute IC, Griffiths SG, Lewis S, Chacko S, et al. Rapid isolation of extracellular vesicles from cell culture and biological fluids using a synthetic peptide with specific affinity for heat shock proteins. PLoS One 2014;9:e110443. https://doi.org/10.1371/journal.pone.0110443.
[13] Helwa I, Cai J, Drewry MD, Zimmerman A, Dinkins MB, Khaled ML, et al. A comparative study of serum exosome isolation using differential ultracentrifugation and three commercial reagents. PLoS One 2017;12:e0170628. https://doi.org/10.1371/journal.pone.0170628.
[14] Van Deun J, Mestdagh P, Sormunen R, Cocquyt V, Vermaelen K, Vandesompele J, et al. The impact of disparate isolation methods for extracellular vesicles on downstream RNA profiling. J Extracell Vesicles 2014;3. https://doi.org/10.3402/jev.v3.24858 24858 [pii].
[15] Lai RC, Tan SS, Yeo RW, Choo AB, Reiner AT, Su Y, et al. MSC secretes at least 3 EV types each with a unique permutation of membrane lipid, protein and RNA. J Extracell Vesicles 2016;5:29828. https://doi.org/10.3402/jev.v5.29828.
[16] Ji H, Chen M, Greening DW, He W, Rai A, Zhang W, et al. Deep sequencing of RNA from three different extracellular vesicle (EV) subtypes released from the human LIM1863 colon cancer cell line uncovers distinct miRNA-enrichment signatures. PLoS One 2014;9:e110314. https://doi.org/10.1371/journal.pone.0110314 PONE-D-14-23898 [pii].
[17] Bradbury A, Pluckthun A. Reproducibility: standardize antibodies used in research. Nature 2015;518:27–9. https://doi.org/10.1038/518027a.
[18] Nakai W, Yoshida T, Diez D, Miyatake Y, Nishibu T, Imawaka N, et al. A novel affinity-based method for the isolation of highly purified extracellular vesicles. Sci Rep 2016;6:33935. https://doi.org/Artn 33935 10.1038/Srep33935.
[19] Popović M, de Marco A. Canonical and selective approaches in exosome purification and their implications for diagnostic accuracy. Transl Cancer Res 2017:S209–25. ⟨https://tcr.amegroups.com/article/view/15820⟩.
[20] Hu M, Kang G, Cheng X, Wang J, Li R, Bai Z, et al. In vitro affinity maturation to improve the efficacy of a hypoxia-inducible factor 1α single-domain intrabody. Biochem Biophys Res Commun 2020;529:936–42. https://doi.org/10.1016/j.bbrc.2020.06.097.
[21] Cheng X, Wang J, Kang G, Hu M, Yuan B, Zhang Y, et al. Homology modeling-based in silico affinity maturation improves the affinity of a nanobody. Int J Mol Sci 2019;20:4187. https://doi.org/10.3390/ijms20174187.
[22] Soler MA, Medagli B, Semrau MS, Storici P, Bajc G, de Marco A, et al. A consensus protocol for the in silico optimisation of antibody fragments. Chem Commun 2019; 55:14043–6. https://doi.org/10.1039/C9CC06182G.
[23] Crépin R, Gentien D, Duché A, Rapinat A, Reyes C, Némati F, et al. Nanobodies against surface biomarkers enable the analysis of tumor genetic heterogeneity in uveal melanoma patient-derived xenografts. Pigment Cell Melanoma Res 2017;30: 317–27. https://doi.org/10.1111/pcmr.12577.
[24] Monegal A, Ami D, Martinelli C, Huang H, Aliprandi M, Capasso P, et al. Immunological applications of single-domain llama recombinant antibodies isolated from a naïve library. Protein Eng Des Sel 2009;22:273–80. https://doi.org/10.1093/protein/gzp002.
[25] Moutel S, Bery N, Bernard V, Keller L, Lemesre E, de Marco A, et al. NaLi-H1: a universal synthetic library of humanized nanobodies providing highly functional antibodies and intrabodies. Elife 2016:5. https://doi.org/10.7554/eLife.16228.
[26] Mandrup OA, Friis NA, Lykkemark S, Just J, Kristensen P. A novel heavy domain antibody library with functionally optimized complementarity determining regions. PLoS One 2013;8. https://doi.org/10.1371/journal.pone.0076834.
[27] Yan J, Li G, Hu Y, Ou W, Wan Y. Construction of a synthetic phage-displayed nanobody library with CDR3 regions randomized by trinucleotide cassettes for diagnostic applications. J Transl Med 2014;12:343. https://doi.org/10.1186/s12967-014-0343-6.
[28] Popovic M, Mazzega E, Toffoletto B, de Marco A. Isolation of anti-extra-cellular vesicle single-domain antibodies by direct panning on vesicle-enriched fractions. Microb Cell Fact 2018;17:6. https://doi.org/10.1186/s12934-017-0856-9.
[29] Prodanović O, Prokopijević M, Spasojević D, Stojanović Ž, Radotić K, Knežević-Jugović ZD, et al. Improved covalent immobilization of horseradish peroxidase on macroporous glycidyl methacrylate-based copolymers. Appl Biochem Biotechnol 2012;168:1288–301. https://doi.org/10.1007/s12010-012-9857-7.
[30] Miletić N, Rohandi R, Vuković Z, Nastasović A, Loos K. Surface modification of macroporous poly (glycidyl methacrylate-co-ethylene glycol dimethacrylate) resins for improved Candida antarctica lipase B immobilization. React Funct Polym 2009; 69:68–75. https://doi.org/10.1016/j.reactfunctpolym.2008.11.001.
[31] Miletić N, Nastasović A, Loos K. Immobilization of biocatalysts for enzymatic polymerizations: possibilities, advantages, applications. Bioresour Technol 2012; 115:126–35. https://doi.org/10.1016/j.biortech.2011.11.054.
[32] Milosavić N, Prodanović R, Jovanović S, Vujčić Z. Immobilization of glucoamylase via its carbohydrate moiety on macroporous poly (GMA-co-EGDMA). Enzyme Microb Technol 2007;40:1422–6. https://doi.org/10.1016/j.enzmictec.2006.10.018.
[33] Prodanović R, Jovanović S, Vujčić Z. Immobilization of invertase on a new type of macroporous glycidyl methacrylate. Biotechnol Lett 2001;23:1171–4. https://doi.org/10.1023/A:1010560911400.
[34] McCaw TR, Koepf EK, Conley L. Evaluation of a novel methacrylate-based protein a resin for the purification of immunoglobulins and Fc-fusion proteins. Biotechnol Prog 2014;30:1125–36. https://doi.org/10.1002/btpr.1951.
[35] Djender S, Schneider A, Beugnet A, Crepin R, Desrumeaux KE, Romani C, et al. Bacterial cytoplasm as an effective cell compartment for producing functional VHH-based affinity reagents and Camelidae IgG-like recombinant antibodies. Microb Cell Fact 2014;13:1–10. https://doi.org/10.1186/s12934-014-0140-1.
[36] Djender S, Beugnet A, Schneider A, de Marco A. The biotechnological applications of recombinant single-domain antibodies are optimized by the C-terminal fusion to the EPEA sequence (C tag). Antibodies 2014;3:182–91. https://doi.org/10.3390/antib3020182.
[37] Veggiani G, Giabbai B, Semrau MS, Medagli B, Riccio V, Bajc G, et al. Comparative analysis of fusion tags used to functionalize recombinant antibodies. Protein Expr Purif 2020;166:105505. https://doi.org/10.1016/j.pep.2019.105505.
[38] Nguyen VD, Hatahet F, Salo KEH, Enlund E, Zhang C, Ruddock LW. Pre-expression of a sulfhydryl oxidase significantly increases the yields of eukaryotic disulfide bond containing proteins expressed in the cytoplasm of E. coli. Microb Cell Fact 2011;10:1–13. https://doi.org/10.1186/1475-2859-10-1.
[39] Veggiani G, de Marco A. Improved quantitative and qualitative production of single-domain intrabodies mediated by the co-expression of Erv1p sulfhydryl oxidase. Protein Expr Purif 2011;79:111–4. https://doi.org/10.1016/j.pep.2011.03.005.
[40] Chabrol E, Charonnat R. Une nouvelle reaction pour l'etude des lipides l'oleidemie. Press Méd 1937;45:1713.
[41] Osteikoetxea X, Balogh A, Szabó-Taylor K, Németh A, Szabó TG, Pálóczi K, et al. Improved characterization of EV preparations based on protein to lipid ratio and lipid properties. PLoS One 2015;10:e0121184. https://doi.org/10.1371/journal.pone.0121184.
[42] Laemmli UK. Cleavage of structural proteins during the assembly of the head of bacteriophage T4. Nature 1970;227:680–5. https://doi.org/10.1038/227680a0.
[43] Jovanović S, Nastasović A, Jovanović N, Jeremic K, Savić Z. The influence of inert component composition on the porous structure of glycidyl methacrylate/ethylene glycol dimethacrylate copolymers. Die Angew Makromol Chemie 2003;219:161–8. https://doi.org/10.1002/apmc.1994.052190113.
[44] Kosaka N, Kogure A, Yamamoto T, Urabe F, Usuba W, Prieto-Vila M, et al. Exploiting the message from cancer: the diagnostic value of extracellular vesicles for clinical applications. Exp Mol Med 2019;51:1–9. https://doi.org/10.1038/s12276-019-0219-1.
[45] Pang B, Zhu Y, Ni J, Thompson J, Malouf D, Bucci J, et al. Extracellular vesicles: the next generation of biomarkers for liquid biopsy-based prostate cancer diagnosis. Theranostics 2020;10:2309–26. https://doi.org/10.7150/thno.39486.
[46] Sahoo S, Adamiak M, Mathiyalagan P, Kenneweg F, Kafert-Kasting S, Thum T. Therapeutic and diagnostic translation of extracellular vesicles in cardiovascular diseases. Circulation 2021;143:1426–49. https://doi.org/10.1161/CIRCULATIONAHA.120.049254.
[47] Coumans FAW, Brisson AR, Buzas EI, Dignat-George F, Drees EEE, El-Andaloussi S, et al. Methodological guidelines to study extracellular vesicles. Circ Res 2017;120: 1632–48. https://doi.org/10.1161/CIRCRESAHA.117.309417.
[48] Théry C, Witwer KW, Aikawa E, Alcaraz MJ, Anderson JD, Andriantsitohaina R, et al. Minimal information for studies of extracellular vesicles 2018 (MISEV2018): a position statement of the International Society for Extracellular Vesicles and update of the MISEV2014 guidelines. J Extracell Vesicles 2018;7:1535750. https://doi.org/10.1080/20013078.2018.1535750.
[49] Koga K, Matsumoto K, Akiyoshi T, Kubo M, Yamanaka N, Tasaki A, et al. Purification, characterization and biological significance of tumor-derived exosomes. Anticancer Res 2005;25:3703–7. ⟨https://ar.iiarjournals.org/content/anticanres/25/6A/3703.full.pdf⟩.
[50] McBride JD, Menocal-Rodriguez L, Candanedo A, Guzman W, Garcia-Contreras M, Badiavas EV. Bone marrow mesenchymal stem cell-derived CD63+ exosomes transport Wnt3a exteriorly and enhance dermal fibroblast proliferation, migration and angiogenesis in vitro. Stem Cells Dev 2017. https://doi.org/10.1089/scd.2017.0087.
[51] Purushothaman A, Bandari SK, Liu J, Mobley JA, Brown EE, Sanderson RD. Fibronectin on the surface of myeloma cell-derived exosomes mediates exosome-cell interactions. J Biol Chem 2016;291:1652–63. https://doi.org/10.1074/jbc.M115.686295.
[52] Caby MP, Lankar D, Vincendeau-Scherrer C, Raposo G, Bonnerot C. Exosomal-like vesicles are present in human blood plasma. Int Immunol 2005;17:879–87. https://doi.org/10.1093/intimm/dxh267.
[53] Bukong TN, Momen-Heravi F, Kodys K, Bala S, Szabo G. Exosomes from hepatitis C infected patients transmit HCV infection and contain Replication competent viral RNA in complex with Ago2-miR122-HSP90. Plos Pathog 2014;10. https://doi.org/ARTNe100442410.1371/journal.ppat.1004424.
[54] Prodanović R, Milosavić NB, Jovanović SM, Vujčić Z. Immobilization of invertase and glucoamylase on a macroporous copolymer of etyleneglycoldimethacrylate and glycidyl methacrylate and potential applications in biotechnology. Hem Ind 2003;57:536–42. https://doi.org/10.2298/HEMIND0311536P.
[55] Spitznagel TM, Clark DS. Surface-density and orientation effects on immobilized antibodies and antibody fragments. Bio Technol 1993;11:825–9. https://doi.org/10.1038/nbt0793-825.
[56] Pardon E, Laeremans T, Triest S, Rasmussen SGF, Wohlkönig A, Ruf A, et al. A general protocol for the generation of Nanobodies for structural biology. Nat Protoc 2014;9:674–93. https://doi.org/10.1038/nprot.2014.039.
[57] Dumoulin M, Conrath K, Van Meirhaeghe A, Meersman F, Heremans K, Frenken LGJ, et al. Single-domain antibody fragments with high conformational stability. Protein Sci 2002;11:500–15. https://doi.org/10.1110/ps.34602.
[58] Monegal A, Olichon A, Bery N, Filleron T, Favre G, de Marco A. Single domain antibodies with VH hallmarks are positively selected during panning of llama

(Lama glama) naïve libraries. Dev Comp Immunol 2012;36:150–6. https://doi.org/10.1016/j.dci.2011.06.016.

[59] Reiner AT, Witwer KW, van Balkom BWM, de Beer J, Brodie C, Corteling RL, et al. Concise review: developing best-practice models for the therapeutic use of extracellular vesicles. Stem Cells Transl Med 2017;6:1730–9. https://doi.org/10.1002/sctm.17-0055.

[60] Brennan K, Martin K, FitzGerald SP, O'Sullivan J, Wu Y, Blanco A, et al. A comparison of methods for the isolation and separation of extracellular vesicles from protein and lipid particles in human serum. Sci Rep 2020;10:1039. https://doi.org/10.1038/s41598-020-57497-7.